Improving the Recyclability of Polymer Composites with Cellulose Nanofibrils

Katie Copenhaver[a*], Bivek Bista[b], Lu Wang[c,d], Samarthya Bhagia[e], Meghan Lamm[a], Xianhui Zhao[f], Mehdi Tajvidi[d], William M. Gramlich[g], Amber M. Hubbard[a], Caitlyn Clarkson[a], Douglas J. Gardner[c,d]

[a]*Manufacturing Science Division, Oak Ridge National Laboratory, 1 Bethel Valley Rd, Oak Ridge, TN 37830, USA.*

[b]*Department of Mechanical Engineering, University of Connecticut, Storrs, CT 06269, USA.*

[c]*Advanced Structures and Composites Center, University of Maine, 160 College Ave, Orono, ME 04469, USA.*

[d]*School of Forest Resources, University of Maine, 160 College Ave, Orono, ME 04469, USA.*

[e]*Biosciences Division, Oak Ridge National Laboratory, 1 Bethel Valley Rd, Oak Ridge, TN 37830, USA.*

[f]*Environmental Sciences Division, Oak Ridge National Laboratory, 1 Bethel Valley Rd, Oak Ridge, TN 37830, USA.*

[g]*Department of Chemistry, University of Maine, 160 College Ave, Orono, ME 04469, USA.*

*Corresponding Author: (K.C.) copenhaverke@ornl.gov

Abstract

Cellulose nanofibers (CNFs) have been widely studied for their reinforcing potential in high-performance composites. While there are numerous publications on CNF-reinforced composites in a variety of polymer matrices, few have considered the recyclability of such thermoplastic composites and whether the incorporation of CNFs deteriorates or improves their performance

upon reprocessing. In this study, two thermoplastic resins, poly(lactic acid) (PLA), and glycol-modified polyethylene terephthalate (PETg), were prepared with CNF reinforcement and thermomechanically recycled to investigate the effect of CNF inclusion on the composite properties after reprocessing as well as their effect on the composites' number of useful life cycles. Changes in mechanical, thermal, rheological, molecular, and microstructural properties of the composites and/or base resins were monitored as a function of cycle numbers. As is typical, the polymers' molecular weight and mechanical performance deteriorated with continued processing. However, the addition of spray dried CNF was found to better maintain the mechanical performance of both polymers throughout multiple recycling steps as compared to neat samples. For example, the tensile strength of PETg with 20 wt.% CNF after 6 processing cycles was found to exceed that of virgin neat PETg, and higher loadings of CNF were found to preserve a higher yield strength during multiple rounds of reprocessing compared to PETg composites with lower CNF loadings. Ultimately this study indicates that the addition of CNF to some thermoplastic materials can increase both their sustainability by offsetting the use of high-embodied energy resins and their circularity by enabling performance retention over more use cycles.

Keywords: nanocellulose, cellulose nanofibrils (CNFs), nanocomposite, biocomposite, poly(lactic acid) (PLA), polyethylene terephthalate-glycol (PETg)

1. Introduction

The growing global dependence on plastics for applications from single use packaging to high-performance composites has led in recent years to a sharp increase in public awareness on the detrimental effects of plastic pollution on global climates and ecosystems. Without the

development of more sustainable materials and recycling practices, the amount of plastic waste entering the world's waterways is predicted to reach 90 million tons per year by 2030.[1] The United States alone generated an estimated 35.7 million tons of plastic waste in 2018, only 8.5% of which was recycled.[2] Increasing pressure from the public as well as government entities has influenced many industries to reduce their dependence on virgin plastic and their output of plastic waste. For this reason, natural fiber-filled thermoplastic composites have gained increasing interest as potential alternatives to common petroleum-based plastics in both commodity and high-performance applications.

Lignocellulosic fibers from a wide variety of sources such as wood, flax, bagasse, hemp, and bamboo, to name a few, have been long studied as reinforcing agents in various polymer matrices.[3-9] These fibers are typically high aspect ratio, being tens of microns to millimeters in length with diameters in the micron range.[10] Cellulose nanofibrils (CNFs) can be extracted from lignocellulosic biomass and have attracted much attention in recent years as reinforcing agents for a new class of high performance, sustainable composite materials. CNFs are most often obtained from wood or other natural fiber sources using existing pulp making equipment and processes, but they can also be derived from such exotic sources as fruit and vegetable skins, shells, and hulls, plant stalks and stems, and even waste cardboard and natural textiles.[11-20] The high aspect ratios (>1 μm in length and <100 nm in diameter [21]) and accordingly high surface areas along with excellent mechanical properties (modulus typically 20-80 GPa and stiffness around 150 GPa [22, 23]) and widespread abundance of CNF sources have made them very appealing for use in composites.[2]

One popular resin reported in literature regarding natural fiber-reinforced composites is polylactic acid (PLA). PLA is a biopolymer typically synthesized from corn or sugarcane products. It has

gained popularity attributable to both its inherent sustainability and its superior mechanical performance and processability.[7, 24] Numerous studies have been reported on the development and optimization of fully bio-based composites using PLA and CNFs [25-29], but few have considered the end-of-life and recyclability of these new materials. A second widely available resin whose recyclability has been well-documented is glycol-modified polyethylene terephthalate (PETg). PETg is a petroleum-derived copolyester of polyethylene terephthalate (PET) that is synthesized by replacing some ethylene glycol with 1,4-cyclohexane dimethanol (CHDM).[30] PETg has been shown to be easily recyclable and can retain its desirable properties over multiple cycles of thermomechanical processing.[31-33] Additionally, there have been numerous reports of recycling PETg-based composites, but these typically employ synthetic fibers such as carbon fiber. [33, 34] Finally, there are no reports to the authors' knowledge that address CNF-reinforced PETg composites and their recyclability.

Recycling of any fiber-reinforced composite is a complicated process, as the fibers and the polymer matrix can degrade after multiple thermomechanical cycles, while other factors such as fiber dispersion, the fiber-polymer interface, and polymer crystallinity may improve.[35-38] The effects of mechanical recycling on the performance of CNF-reinforced composites warrants further investigation before these materials can be widely promoted as sustainable, eco-friendly composites. In this study, the effects of multiple grinding and injection molding (IM) processes on the mechanical, thermal, rheological, and morphological properties of CNF-reinforced thermoplastic composites using PLA and PETg were evaluated. The performance of both neat and CNF-reinforced PLA and PETg after repeated reprocessing steps is herein compared to assess the recyclability and overall sustainability of both composite materials.

2. Materials and Methods

2.1. Materials

Poly(L-lactide) (Ingeo 4043D), referred to as PLA in this work, was purchased from NatureWorks, LLC (Minnetonka, Minnesota), and PETg (HiFill PETg 1704 3DP) was purchased from Techmer PM, LLC (Clinton, TN). CNF slurry was provided by the University of Maine's Process Development Center. The CNFs were refined to 90% fines (amount of material in the sample with dimensions <200 μm) from northern bleached softwood Kraft pulp on a single disk refiner and spray dried on the pilot scale (GEA-Niro, Germany) using methods previously reported.[39]

2.2. Composite preparation

2.2.1. Compounding and grinding

Before compounding, spray dried CNFs were oven dried at 105 °C, and PETg/PLA pellets were oven dried at 60 °C for a minimum of 4 hours. A masterbatch containing 20 wt.% CNFs was prepared by feeding a mixture of spray dried fibrils and PETg or PLA granulate into a twin screw co-rotating extruder (herein referred to as PETg20CNF and PLA20CNF, respectively; C. W. Brabender Instruments, South Hackensack, NJ) attached to a drive system (Intelli-Torque Plastic-Corder). The extruder was operated at 180 °C for all heat zones and a 30-rpm screw speed for PLA/CNF mixtures, while PETG/CNF mixtures were processed at 230 °C with a 30-rpm screw speed. The extrudate was granulated by a grinder. Some of the granulate was then mixed with neat PETg or PLA pellets to dilute the mixtures and produce new materials containing 5 wt.% CNFs (PETg5CNF and PLA5CNF, respectively). The 5 wt.% CNF composites were subjected to extrusion and grinding at the same conditions as their 20 wt.% CNF composite counterparts.

2.2.2. Injection molding and recycling

Prior to IM, granulate from the four composite formulations as well as neat PLA and PETg was oven dried at 60 °C for 4 hours. Each formulation was formed into flexural and tensile bars (flexural bars machined to impact bars according to ASTM D256-10, tensile bars according to ASTM D638, Type I) using a Mini-Jector Model #50 injection molder (Miniature Plastic Molding, Farmington Hills, MI) with a ram pressure of 17 MPa at 190 °C for PLA and PLA/CNF and 230 °C for PETg and PETg/CNF. The mold was kept at 30 °C, and samples were held 10 seconds before demolding (cycle #1). After the first IM cycle, samples were allowed to cool for two days while the remaining material from each formulation was ground, oven dried, and injection molded using identical conditions described previously. This process was repeated for each formulation up to 6 times (7 cycles total). However, on the 7th IM cycle using PLA20CNF, the material was observed to be flowing continuously out of the injection nozzle before the cycle started, indicating that the material viscosity was too low to be processed effectively at the given conditions. The temperature of the IM unit was thus lowered to 175 °C for the 7th cycle performed with PLA20CNF. Both PLA and PETg were subjected to 3 cycles for neat resins and composites with 5 wt.% CNF. Since the effect of recycling on fiber-reinforced composites is typically more pronounced with increased fiber loading, composites with 20 wt.% CNF were subjected to addition cycles (7 cycles total) to elicit the most distinct effects. In each characterization step, all samples (neat and composite) from all 3 cycles were tested, and additional samples from 7th processing cycle were tested for composites with 20 wt.% CNF.

2.3. Characterization

2.3.1. Mechanical Properties

2.3.1.1. Tensile

Tensile tests were performed using an electromechanical testing machine according to the procedures outline in ASTM D 638-14. Before the test, the samples were kept in a temperature (23±2°C) and humidity (50±10% RH) controlled room for 1-2 days. The original dimensions of the tensile bars were recorded before the start of each test and an extensometer was connected after the sample was clamped to measure the dimensional changes as the test was performed. Tests using neat and composite PLA samples were performed until the sample broke, while tests using neat and composite PETg samples were performed until the stress-strain curves plateaued and significant yielding was observed. At least 8 samples were tested for each formulation and processing cycle, and average values of tensile strength and modulus and their standard deviation were reported for each property.

2.3.1.2. Impact

Impact tests were performed using a Ceast pendulum impact tester (Model Resil 50B). The molded flexural bars were cut into impact bars and notched according to ASTM D256-10 (Izod Pendulum impact). The original dimensions of each sample were recorded, and the impact bars were kept in a temperature-controlled room for 1-2 days before testing was performed. Samples from the first 3 cycles of each specimen type along with samples from the 7^{th} cycle of the composites with 20 wt.% CNF were subjected to impact testing. At least 7 samples from each formulation were tested to calculate their average and standard deviation.

2.3.2. Scanning Electron Microscopy (SEM)

The fracture surfaces of composites samples with 20 wt.% CNF from the first and 7th processing cycles after tensile testing were sputtered with iridium and imaged with a Zeiss Merlin field emission SEM in secondary electron mode at an accelerating voltage of 1kV.

2.3.3. Molecular weight measurements (GPC and NMR)

Gel permeation chromatography (GPC) was carried out to determine the molecular weights of PLA in samples. Samples were cut into small pieces and placed into scintillation vials with tetrahydrofuran (THF) overnight with magnetic stirring and then passed through a 0.22 μm PTFE filter. GPC was carried out on an Agilent Technologies 1260 Inifinity Series GPC/SEC system with three Phenogel columns in series with 50, 103, and 106 Å pore sizes and a refractive index detector at 35 °C. THF was used as the mobile phase with a flow rate of 1 mL/min. The system was calibrated with linear polystyrene standards, and the baseline correction and peak integration were performed using the Agilent GPC/SEC Polymer Analysis software.

PETg samples were analyzed by a trichloroacetyl isocyanate (TAI) derivatization nuclear magnetic resonance (NMR) technique.[40] Samples were dissolved in deuterated chloroform ($CDCl_3$) overnight, and then 5 μL of TAI was added to 600 μL of NMR solvent. ^{1}H NMR was carried out using 90° pulse in Bruker Avance 500 MHz NMR with a broadband cryoprobe for 1024 scans. Number-average molecular weights were calculated based on the ratio of the concentration of aromatic protons and OH and COOH end groups.

For both polymer matrices, the molecular weight of composite samples with 20 wt.% CNF from cycles 1-3 and cycle 7 was measured. The molecular weight of the neat polymer after the initial processing cycle (cycle 1) was also measured for reference.

2.3.4. Rheology

Rheological analyses were conducted using a Discovery HR-3 (TA Instruments, New Castle, DE) with 25 mm parallel plates at a gap of 1 mm. A temperature of 180 °C was used with neat and composite PLA samples while a temperature of 220 °C was used with neat and composite PETg samples. Oscillatory strain amplitude sweeps were first performed on each type of sample to identify a strain value within its linear viscoelastic region. Frequency sweeps were then performed on each type of sample using the corresponding temperature and strain values. The storage and loss moduli and complex viscosity of each sample were recorded at a frequency range of 1 to 100 rad/s. Steady shear tests were also performed on each sample. The viscosity was recorded for each material at a shear rate of 0.1 to 1000 s^{-1} at 180 °C for PLA samples and 220 °C for PETg samples. Samples from the first 3 cycles of each specimen type along with samples from the 7^{th} cycle of the composites with 20 wt.% CNF were subjected to rheological testing. Each test was performed twice to ensure repeatability.

2.3.5. Thermal

2.3.5.1. Differential Scanning Calorimetry (DSC)

DSC tests were performed on a DSC 2500 (TA Instruments, New Castle, DE) using a heat-cool-heat-cool method. The test samples were cut from tensile or flexural bars, each weighing 6-9 mg. The neat and composite PLA and PETg samples were equilibrated at 40 °C, heated to 180 °C at a rate of 10 °C/min., held isothermally for 1 minute, cooled to 40 °C at a rate of 10 °C/min, held isothermally for 1 minute, and finally heated back to 180 °C at 10 °C/min. The same procedure was followed for neat and PETg samples with an upper temperature of 220 °C.

The glass transition temperature (T_g), melting temperature (T_m) enthalpy of cold crystallization (ΔH_{cc}), (cold) crystallization temperature (T_c), and enthalpy of melting (ΔH_m) were obtained from the second heating curve of each sample. The crystallization temperature (T_c) and enthalpy of crystallization (ΔH_c) were obtained from the first cooling curve of PETg samples. In samples exhibiting crystallization, the degree of crystallization was calculated using the first and second heating curves and equation:

$$X_c = \frac{\Delta H_m - \Delta H_{cc}}{w * \Delta H_0} \qquad (1)$$

in which ΔH_m is the melting enthalpy and ΔH_{cc} is the cold crystallization enthalpy, while ΔH_0 is the melting enthalpy for 100% crystalline PLA or PETg. The value of ΔH_0 used in these calculations for PLA samples 93 J/g, while 88 J/g was used for PETg samples.[30, 41] Finally, *w* is the weight fraction of PLA or PETg in the sample. Samples from the first 3 cycles of each specimen type along with samples from the 7th cycle of the composites with 20 wt.% CNF were tested (20 samples total). Each test was performed twice to ensure repeatability.

2.3.5.2. Thermogravimetric Analysis (TGA)

TGA experiments were carried out on a TGA Q500 (TA Instruments, New Castle, DE). Test samples weighing 3-5 mg were placed in platinum pans and heated from room temperature to 600 °C at a rate of 10 °C/min in a nitrogen atmosphere. Samples from the first 3 cycles of each specimen type along with samples from the 7th cycle of the composites with 20 wt.% CNF were tested. Each test was performed twice to ensure repeatability.

2.3.6. Degradation analyses (NMR and XRD)

2.3.6.1. NMR

PLA and PETg composites with 20 wt.% CNF from process cycles 1 and 7 were dissolved in $CDCl_3$ (7.26 ppm ^1H, 77.16 ppm ^{13}C) overnight. The liquid phase was filtered and put into 5 mm NMR tubes. NMR spectroscopy was carried out using a Bruker Avance 500 MHz NMR with a cryoprobe. Shifts were calibrated using solvent residual peaks. ^1H spectra were acquired with zg 90˚ pulse, 14.99 ppm spectral width, 2.18 sec acquisition time, 4 sec delay time and 128 scans. ^{13}C spectra were acquired with zgpg pulse, 233.8 ppm spectral width, 0.557 sec acquisition time, 1 sec delay time and 6144 scans.

2.3.6.2. X-ray Diffraction (XRD)

XRD was performed on PETg20CNF composites from process cycles 1 and 7 using a Panalytical Empyrean diffractometer with copper Kα radiation operating at 45 kV and 40 mA in the range of 5-90 °2θ.

3. Results and discussion

The effects of recycling on the mechanical performance of a polymer or polymer composite can often be related to fiber attrition and a loss of aspect ratio, enhanced fiber dispersion, and changes in polymer/fiber interactions, crystallinity, and the polymer's molecular weight, among others. These factors can negatively or positively impact the material's mechanical performance, and at times can effectively counteract one another resulting in no measurable change in mechanical and other properties. The relationships between the aforementioned composite properties and its performance after recycling can be complex but have been thoroughly documented and discussed in literature in the field of natural fiber-reinforced composites.[36, 42-45] The recycling of thermoplastic composites reinforced with spray dried CNF, however, has not yet been studied.

To evaluate the effects of thermomechanical recycling on PLA and PETg composites reinforced with spray dried CNF, the mechanical performance (impact and tensile properties) of neat and composite samples at 5 and 20 wt.% loading of CNF was first measured after initial extrusion and two successive recycling steps. Composites with the higher CNF concentration were further probed to determine the number of cycles either composite could withstand before significant property loss. Samples were continuously reprocessed until a 30% deterioration in any of their mechanical properties was measured, which was determined to be four additional recycling steps.

3.1. Mechanical properties

Neat and composite PLA and PETg samples with varying loading levels of CNF were subjected to tensile testing after IM (cycle 1) and recycling via grinding and IM (cycles 2-7). Results of tensile tests are shown Figure 1, and the changes in yield strength and modulus of each sample after 3 and 7 processing steps are quantified in

Table 1. Impact testing results are shown in Figure S1 of the supporting information (SI).

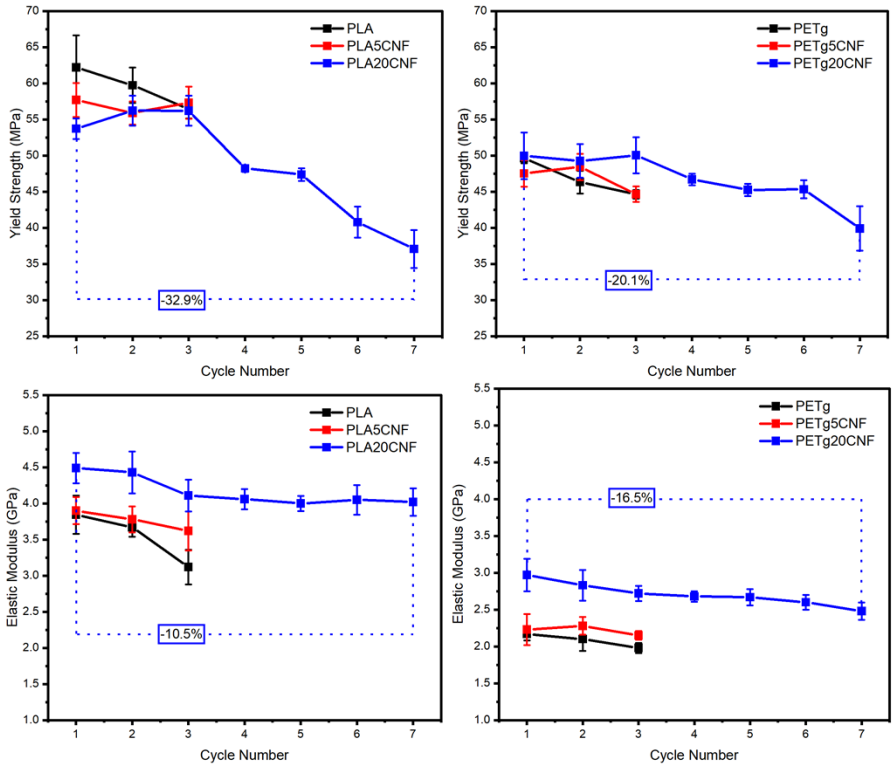

Figure 1. Tensile performance of neat and composite samples

Table 1. Changes in tensile performance of neat and composite samples after 3 and 7 processing cycles

Sample	Δ Yield strength after 3 cycles (%)	Δ Yield strength after 7 cycles (%)	Δ Elastic modulus after 3 cycles (%)	Δ Elastic modulus after 7 cycles (%)
Neat PLA	-9.3		-0.1	
PLA5CNF	-0.6		-7.2	
PLA20CNF	+4.6	-31.0	-8.5	-10.5
Neat PETg	-10.1		-8.8	
PETg5CNF	-6.0		-3.6	
PETg20CNF	+0.2	-20.1	-8.4	-16.5

The mechanical performance of both the neat and composite samples generally deteriorates with recycling, which is most evident in the samples subjected to 7 thermomechanical cycles. A loss in tensile performance upon recycling is commonly seen in thermoplastics and thermoplastic composites and is primarily attributed to degradation of the polymer matrices, changes in fiber aspect ratios or their dispersion, and deterioration of the polymer/fiber interface.[42] Polymer

degradation or a loss in molecular weight after mechanical recycling has been demonstrated in natural and synthetic polymers both semicrystalline and amorphous.[3, 35, 37] Furthermore, the presence of fibers or fillers in a composite result in higher shear forces within the material during thermomechanical processing, which can exacerbate the degradation of the polymer matrix.[42, 46] An increase in the stiffness and accompanying decrease in tensile strength upon addition of spray dried CNF has been previously reported.[47-49] Spray drying of CNF leads to agglomeration to particles with a low aspect ratio and wide size distribution, and the incorporation of the hydrophilic CNF aggregates into a hydrophobic PLA matrix can result in areas of stress concentration, leading to premature failure under tensile stress and a lower yield strength with increased particle loading.[49-52]

In the neat and composite PLA samples, the elastic modulus steadily decreases upon reprocessing. The yield strength of the neat PLA similarly decreases with successive recycling steps. Deterioration of the elastic modulus and strength of the neat polymer samples is attributable to a degradation of the polymer matrices resulting from thermomechanical cycling. The tensile strength of the PLA/CNF composite samples, on the other hand, initially remains constant (within error) in the sample with the higher CNF concentration. The spray dried CNF aggregates are unlikely to have broken up to smaller particles or individual fibrils during reprocessing because of the high degree of hydrogen bonding within the particles, but the retention of tensile strength during the initial recycling stages could signify improved mixing or distribution of the CNF particles that mitigates the negative effects of a deteriorating polymer matrix on the composite strength. However, a significant loss of tensile strength is observed after 7 processing cycles of the PLA20CNF samples, again likely attributable to excessive polymer degradation.

The trends in tensile elastic modulus and strength of PETg and PETg/CNF composites after recycling are similar to that of their PLA counterparts. Neat PETg exhibited yielding and necking before fracture, while all the PETg composite samples exhibited brittle fracture. The tensile strength of the composite samples remains nearly constant in the first three thermomechanical cycles while the strength of the neat polymer decreases; essentially, the CNF concentration and mechanical property retention is directly related, again indicating a reinforcing effect of the CNF particles. The tensile strength of PETg20CNF is lowered by approximately 20% after 7 processing cycles. However, the strength of this composite after 6 processing cycles is nearly identical to that of neat PETg after only 3 processing cycles, indicating that the addition of CNF improves the recyclability of the material, extending its number of functional lifetimes or use cycles. Additionally, the tensile elastic modulus of both PLA and PETg composites with 20 wt.% CNF after 7 process cycles remains higher than that of the neat resins. Depending on the application, this data suggests that PETg can withstand recycling better than PLA in terms of mechanical performance, and the effects of thermomechanical recycling on either resin can be diminished with the addition of spray dried CNF.

The impact strength of each neat and composite sample, shown in the SI (Figure S1), remains relatively stable throughout recycling, even up to seven cycles. Recycling of natural fiber-reinforced composites has been shown by some researchers to improve their impact strength, theorizing that deterioration of a polymer matrix and fiber breakup render the composite more ductile and able to absorb more energy upon impact.[38, 42, 46] Competing factors such as increased ductility and improved particle dispersion throughout recycling steps could have led to the retention in impact strength observed in both PLA and PETg samples.

3.2. SEM

The fracture surfaces of the PLA and PETg composites with 20 wt.% of CNF particles were each imaged using SEM after the first and seventh process cycles to visualize morphological changes in the most heavily processed samples. Images of each sample are shown in Figure 2.

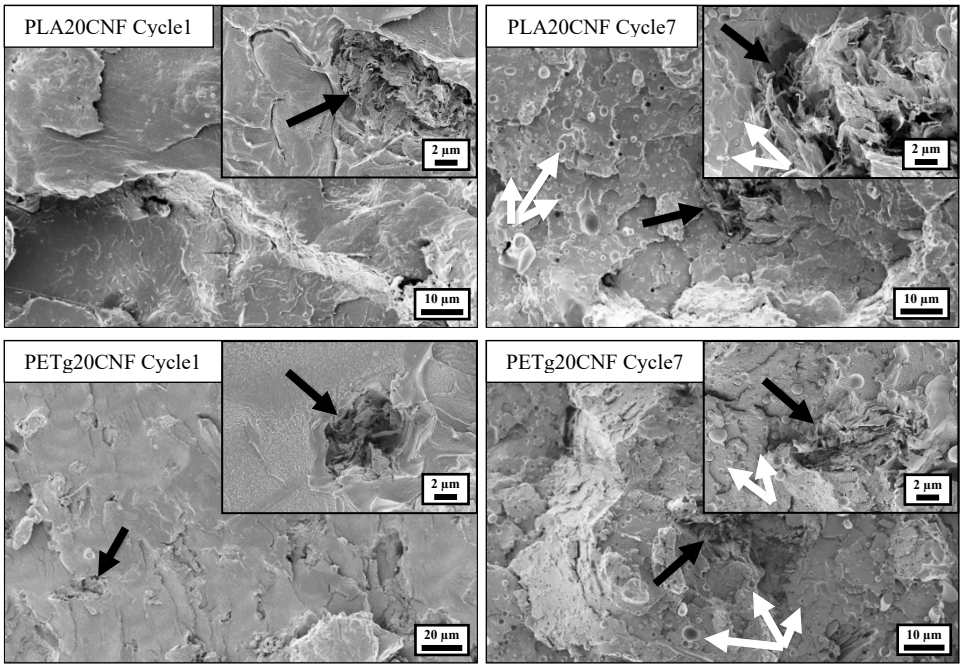

Figure 2. Fracture surfaces of PLA and PETg composites with 20 wt.% CNF particles (black arrows indicate CNF particles, white arrows indicate porosity)

Each image shown in Figure 2 displays agglomerated CNF particles embedded in the composites, indicated by black arrows. These particles appear similar to other thermoplastic composites with spray dried CNF seen in literature.[47, 53] The polymer matrix does not appear to have penetrated the fibril bundles, regardless of the polymer type or number of processing cycles. Additionally, the particles appear to have remained intact throughout the recycling process, indicating that the shear imposed on the CNF particles during thermomechanical processing was not sufficient to

overcome the interfibrillar bonds formed during spray drying attributable to hornification of the nanofibrils.[50-52] As such, the aspect ratio and dispersion of the particles likely remained constant throughout recycling.

The most noticeable difference between the images of both composites from the first and seventh processing cycles is the appearance of a high degree of porosity after recycling, indicated by white arrows in Figure 2. This porosity could be indicative of degradation of each polymer matrix as reflected in the tensile properties shown above. Chain scission during thermomechanical processing can form byproducts such as carbon dioxide and water, among others, which could offgas and result in the pores seen in Figure 2.[32] Additionally, as some macro- or microscale porosity can be introduced during IM, repeated cycling and reinjection of materials causes porosity to build up in the samples. This porosity is also likely a significant contribution to the deterioration of the tensile strength in both the PLA- and PETg20CNF samples after 7 processing cycles, as pores act as further points of stress concentration and early failure under tensile strain.[54]

3.3. Molecular weight and rheological behavior

The molecular weight of the neat polymers and composite samples with 20 wt.% CNF at cycles 1, 2, 3, and 7 were measured using GPC for PLA samples and NMR for PETg samples. NMR was used for PETg samples because of compatibility issues between the GPC and the solvent needed to dissolve PETg. As such, only the number-average molecular weight (M_n) of the PETg samples were measured in this study. M_n of each sample measured is plotted as a function of cycle number in Figure 3. These values along with the weight-average molecular weight (M_w) and dispersity index (Đ) of the PLA samples are given in the SI (Table S1).

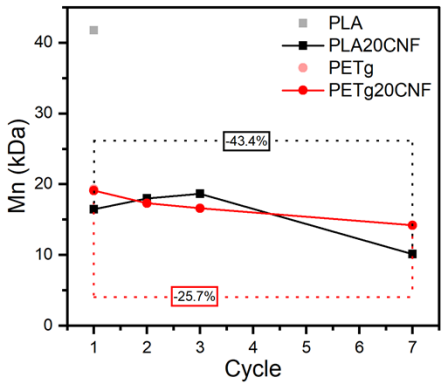

Figure 3. Number-average molecular weight of select neat and composite samples

An initial loss in molecular weight can be observed between the neat and composite samples after IM (and compounding for the composite sample, cycle 1), significantly more so in PLA than in PETg. PLA experiences a reduction from 41.8 to 16.5 kDa between the neat IM sample and the composite IM sample (both cycle 1), while PETg only changes from 19.3 to 19.1 kDa (neat IM and composite IM, respectively, which is difficult to see in Figure 3, as the points for the first cycle of PETg and PETg20CNF are nearly identical). Reduction of a polymer's molecular weight upon thermomechanical processing is attributed to chain scission and can be exacerbated if the material is not fully dried before compounding. PLA is known for being particularly susceptible to hydrolytic degradation at high temperatures.[55, 56] Additionally, natural fibers such as cellulose are hygroscopic and can retain moisture even after rigorous drying before compounding.[42, 55, 57, 58] The drastic reduction in M_n in PLA between the neat and composite samples in cycle 1 could be attributed to residual moisture in the CNF present during compounding, which adversely affected the PLA more than the PETg. With repeated recycling, the molecular weight of both composites continuously decreases. The trends in the M_n of both composites are nearly linear, although the loss of molecular weight in PLA is more rapid than that of PETg, signifying that the molecular structure of PETg is more stable and can withstand more thermomechanical processing

than PLA. The steady decrease in M_n of both composites with successive reprocessing cycles also reflects the declining tensile behavior shown in Figure 1.

The frequency- and rate-dependent viscoelastic behavior of neat and composite samples was then measured using a parallel plate rheometer. Plots of the frequency-dependent storage and loss moduli and complex viscosity as well as the shear rate-dependent viscosity are given in the SI (Figures S2 and S3). The rheological behavior of the neat and composite samples generally follows the trends of decreasing molecular weight and mechanical performance with repeated recycling. The storage and loss moduli and complex and shear viscosities of each sample show a decreasing trend, which can be attributed to the loss in molecular weight after each process cycle. All samples exhibited shear thinning behavior, and in both materials the highest degree of shear thinning (*i.e.*, steepest slope in viscosity vs. shear rate in the shear thinning region) is observed in the composites with a higher particle loading. Inflections in the curves of viscosity as a function of shear rate can be observed at higher shear rates in both PLA and PETg with increasing filler content, indicating that the inclusion of fillers slightly stabilizes the materials against shear thinning.

3.4. Thermal properties

The thermal behavior of neat and composite samples was then measured using DSC and TGA. Results from DSC tests including thermal transition temperatures and the degree of crystallinity in each sample are shown in Figure 4. The thermal transition temperatures and crystallinity of each sample as well as TGA plots found in the SI (Table S2 and Figure S4, respectively).

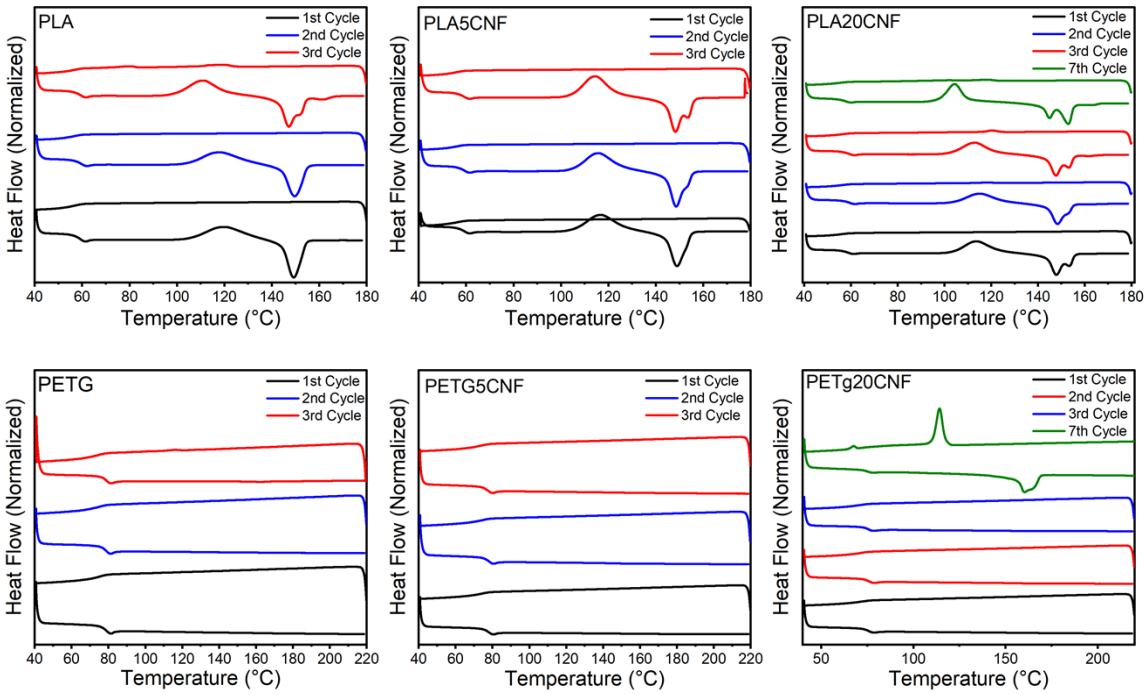

Figure 4. DSC traces of neat and composite samples

In all PLA samples, the thermal transitions shift to lower temperatures with repeated reprocessing. This trend is most noticeable in the cold crystallization temperatures. The temperature at which the glass transition, cold crystallization, and melting occurs in a polymer sample depends on the energy required for polymer chains to diffuse. A reduction in the molecular weight upon recycling, as seen above, increases the mobility of polymer chains and can allow them to crystallize or melt at lower temperatures.[42, 59, 60] The degree of crystallinity within each neat and composite PLA sample, listed in Table S2, also increases upon recycling, which can again be attributed to a loss in molecular weight leading to increased mobility of polymer chains. These trends are similar in both the first and second heats. The crystalline content of the 20 wt.% composite PLA samples is higher than their neat and 5 wt.% composite counterparts. The higher filler content of the 20 wt.% CNF samples would have caused more shear and hydrolysis within the samples during thermomechanical processing and accelerated the degradation of PLA, leading to a higher

crystallinity in the PLA20CNF samples as compared to PLA5CNF. The increase in crystallinity upon recycling likely positively impacted the materials' mechanical performance, facilitating a retention of mechanical properties during successive reprocessing cycles. A higher degree of polymer degradation and accompanying crystallinity in polymer composites with higher filler loading has also been noted by numerous researchers.[42, 61]

As depicted in Figure 4, the melting peaks of the neat and 5 wt.% CNF composites PLA samples splits into two peaks upon recycling, indicating the emergence of a second crystalline phase or the formation of more stable or perfect crystals (i.e., melt recrystallization). This phenomenon has been documented by numerous authors and can be related to the decrease in the molecular weight of PLA upon recycling.[8, 55, 62] Shorter polymer chains within the sample are more mobile and therefore able to organize themselves into more stable crystals that require a higher temperature to melt. PLA20CNF exhibits a double melting peak at each cycle number, but the magnitude of the second peak increases relative to that of the first upon recycling, reflecting the molecular weight data in Figure 3**Error! Reference source not found.**.

The TGA traces of each PLA and PETg sample (SI, Figure S4) show little change after recycling. The onset of degradation can be observed to shift to slightly lower temperatures with successive reprocessing steps, with the largest change noticeable in both the PLA and PETg samples with 20 wt.% CNF after 7 processing cycles. The onset of degradation shifts to lower temperatures with increasing CNF content, reflecting the lower thermal stability of cellulose in comparison to that of PLA and PETg. While the majority of the neat PLA sample degrades by 350 °C, the addition of CNF to the samples results in a second degradation step between 350 and 450 °C. The residual weight at 350 °C also increases with increasing CNF content. In neat PETg, approximately 90% of the sample degrades in a single degradation step between 360 and 420 °C. In the composite

PETg samples, a small, initial degradation step beginning around 300 ℃ can be observed, corresponding to an approximate 5 and 20% weight loss in the PETg samples with 5 and 20 wt.% CNF, respectively, clearly indicating the degradation of cellulose prior to the degradation of PETg. The initial weight loss step in the PETg20CNF sample after 7 processing steps exceeds 20%, however, which could be attributable to the degradation of lower molecular weight species generated during successive recycling steps.

PETg is an amorphous polymer and, as such, shows no crystallization or melting transitions in a typical DSC scan.[31] The neat and 5 wt.% CNF composite PETg samples show no activity on DSC scans up to 220 °C aside from a glass transition, and the T_g of both sample sets stays relatively constant throughout three thermomechanical cycles. PETg20CNF, however, shows a significant decrease in T_g as well as clear melting and crystallization peaks in the sample reprocessed 7 times. Crystallization within PETg is rarely reported in literature, even in studies on repeated recycling of PETg and its composites for 3D printing.[32, 33] Furthermore, most reported crystallization in PETg in literature is induced via chain alignment under strain [30, 31, 63] or by altering its composition (namely, the ratio of ethylene glycol to CHDM used in synthesis).[64, 65] The reported crystallinity of the PETg sample with 20 wt.% CNF after 7 processing cycles was calculated using melting enthalpy for 100% crystalline PETg from literature calculated via XRD and DSC comparison of strain-induced crystalline PETg samples.[30, 41] It was shown through NMR measurements that the molecular weight of the PETg composites decreases throughout recycling, so it is possible that some polymer chains gained sufficient mobility upon shortening to be able to crystallize. Vidakis, et al., also observed potential crystallization of PETg after multiple recycling steps indicated by a reduction in the intensity of Raman bands attributed to a conversion of amorphous gauche ethylene glycol group conformers to crystalline trans conformers.[32]

Further characterization was performed on PETg20CNF samples from cycles 1 and 7 to investigate this unexpected crystallization.

3.5. NMR and XRD

Composite samples with 20 wt.% CNF from cycles 1 and 7 were further analyzed using x-ray diffraction and NMR. ^{1}H spectra from NMR analyses of PLA from composites at process cycles 1 and 7 are shown in Figure 5. For PLA cycle 1 and cycle 7, peaks at 1.56 (CH_3) and 5.19 ppm (CH) represent poly(L-lactide) polymer (PLLA). Because of the presence of minor quantities of D-lactide isomer, peaks on either side of the main methyl and methine peaks were observed in ^{1}H spectra.[66] The CH_3, CH and C=O carbon peaks in ^{13}C spectra appeared at 16.76, 69.14 and 169.72 ppm, respectively, which is shown in Figure S6 of the SI. Comparison between the traces of cycle 1 and 7 indicate that recycling cleaved ester bonds in PLA into –COOH and –OH end groups.[67]

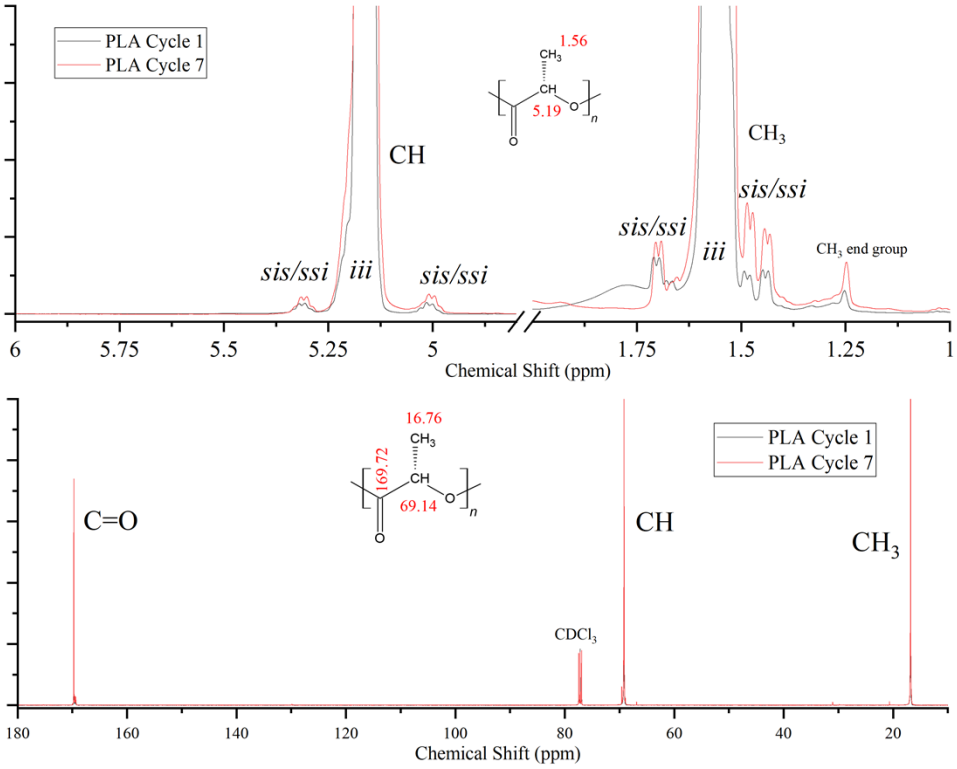

Figure 5. Top: ^{1}H NMR spectra of PLA with ~4% poly(D-lactide). iii represents main signal from L-lactide repeating units from isotactic pairwise relationship sis/ssi satellite signals represent syndiotactic and isotactic pairwise relationships due to presence of PDLA. Bottom: ^{13}C spectra of PLA

^{1}H and ^{13}C spectra from analysis of PETg from composites at process cycles 1 and 7, shown in Figure 6, identified peaks corresponding to terephthalic acid (TA), ethylene glycol (EG) and cyclohexanedimethanol (CHDM) monomers. The ratio of cis(c)/trans(t) PETg isomers, calculated from oxymethyelene protons of CHDM (5(*c*)/5(*t*) at 4.29/4.18 ppm) was 32/68 which is close to the 30/70 molar ratio for commercial PETg. Furthermore, the ratio of CHDM/EG from 5(c)+5(t)/4 ((4.29+4.18)/4.69 ppm) was 31/69 which is close to the 30/70 ratio reported for commercial PETg.[68]

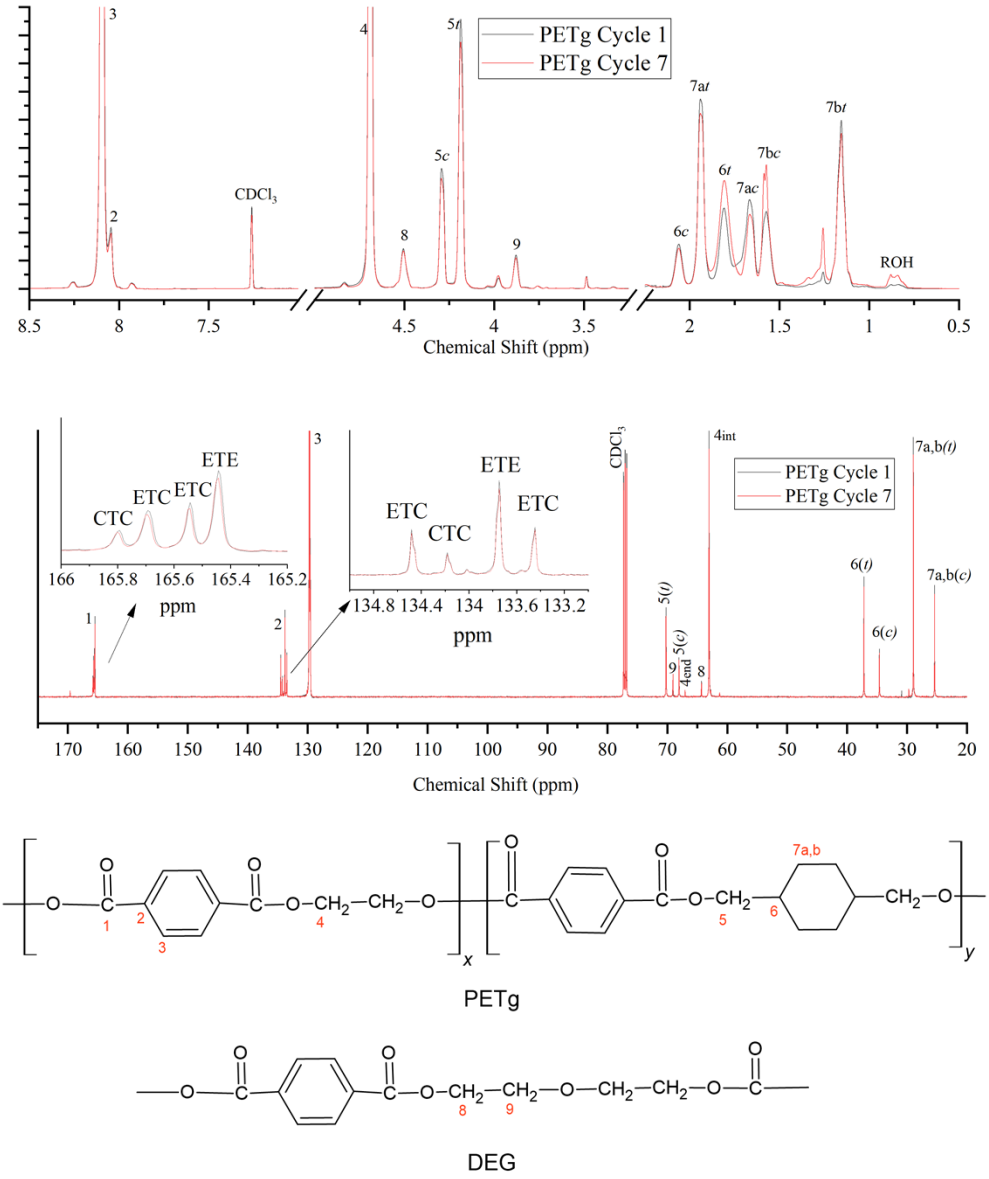

Figure 6. Top: ^{1}H NMR spectra of PETg. Middle: ^{13}C spectra of PETg. Bottom: chemical structures of PETg. DEG=diethylene glycol

The dyad sequence of ethylene (E) terephthalate (T) and glycol (C (CHDM)) terephthalate monomers in the PETg samples was determined using the following equations:

$$\eta_{ET} = \frac{I_{ETE} + {}^{I_{ETC}}/_{2}}{{}^{I_{ETC}}/_{2}} \quad (2)$$

$$\eta_{CT} = \frac{I_{CTC} + {}^{I_{ETC}}/_{2}}{{}^{I_{ETC}}/_{2}} \quad (3)$$

$$R = {}^{1}/_{\eta_{ET}} + {}^{1}/_{\eta_{CT}} \quad (4)$$

In the above equations, η_{ET} and η_{CT} refer to the average sequence lengths of ET and CT monomers, respectively, R refers to the degree of randomness, and I_{ETE}, I_{ETC}, and I_{CTC} are integrals of quaternary carbons of TA (133.45–134.48 ppm).[69] The values of $\eta_{ET,}$ η_{CT} and R were 3.09, 1.48 and 0.993 for cycle 1 and 2.98, 1.47 and 1.00 for cycle 7, which are close to the 3.5, 1.4 and 1 theoretical values for 30/70 ratio of CHDM/EG.[69] The R value close to 1 indicates that the PETg used in this study is a random copolyester. The absence of peaks at 100.4 and 140.8 ppm in the ^{13}C spectra of Cycle 7 reveals that vinyl end groups were not formed due to recycling degradation, and cleavage only resulted in formation of –COOH and –OH end groups. Finally, the peaks at 4.50 and 3.88 ppm in the ^{1}H spectra and 64.3 and 69.3 ppm in the ^{13}C spectra indicate presence of diethylene glycol (DEG) group that is commonly found in commercial PET and PETg polymers.[68, 70] The chemical shifts and corresponding assignments from analysis of the PETg samples are listed in Table S3 of the SI.

XRD spectra of PETg composite samples are shown in Figure 7. The XRD spectra of composite PETg/CNF samples from process cycles 1 and 7 appear similar. CNF typically exhibits characteristic peaks of cellulose I around 15°, 22°, and 35°, making other peaks in that range difficult to discern.[71, 72] However, two peaks close to 14° and 17° are observed in the heavily recycled PETg composite sample. These peaks have also been reported in XRD spectra of PET, suggesting that the degraded crystalline product of heavily recycled PETg is similar in structure to

PET.[64, 73, 74] The low intensity of these peaks is expected, as the crystallinity calculated from DSC measurements, listed in **Error! Reference source not found.**, is also low.

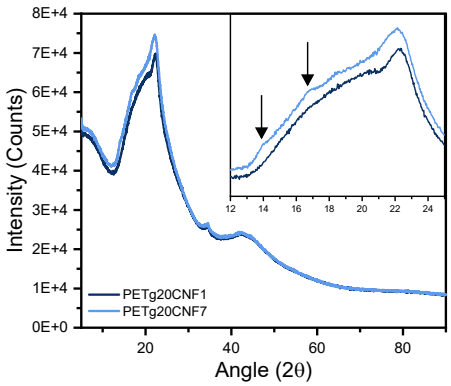

Figure 7. XRD spectra of PETg/20 wt.% CNF from cycles 1 and 7

4. Conclusions

Deterioration of the tensile performance of PLA and PETg composites with 5 and 20 wt.% CNF was observed after thermomechanical recycling. These changes in performance were explained by both SEM, in which porosity is observed to increase with recycling, and molecular weight analyses showing decreases in both polymers' molecular weights upon reprocessing. In the PETg samples, crystallinity was surprisingly exhibited in the composite sample with 20 wt.% CNF after 7 thermomechanical cycles, which prompted further study via NMR and XRD. These studies indicated that the degradation of PETg upon recycling enabled crystallization within the typically amorphous polymer, likely from degraded polymer chains with structures similar to that of PET. Based on the mechanical performance of the neat and composite samples in this study, it can be inferred that the addition of spray dried CNF maintains the mechanical performance of both polymers during recycling, particularly in the first 3 thermomechanical cycles. For example, the yield strength of PETg20CNF after 6 thermomechanical cycles is nearly identical to that of neat

PETg and PETg with 5 wt.% CNF after 3 thermomechanical cycles, meaning the number of useful lifetimes of PETg could be doubled with sufficient CNF inclusion for applications in which tensile strength is an important performance metric. This study indicates that the addition of CNF to some polymer materials can not only increase their sustainability (*e.g.*, offsetting the use of petroleum-derived resins), but also increases their circularity by enabling performance retention over more numerous life cycles.

Funding: The authors acknowledge the support from the US Department of Energy (DOE) Advanced Materials and Manufacturing Technologies Office and used resources at the Manufacturing Demonstration Facility at Oak Ridge National Laboratory, a User Facility of DOE's Office of Energy Efficiency and Renewable Energy. This manuscript has been authored by UT-Battelle, LLC under CPS 848 Agreement 35714 with the U.S. Department of Energy. The United States Government retains and the publisher, by accepting the article for publication, acknowledges that the United States Government retains a nonexclusive, paid-up, irrevocable, worldwide license to publish or reproduce the published form of this manuscript, or allow others to do so, for United States Government purposes. The Department of Energy will provide public access to these results of federally sponsored research in accordance with the DOE Public Access Plan (http://energy.gov/downloads/doe-public-access-plan).

References

[1] S. B. Borrelle *et al.*, "Predicted growth in plastic waste exceeds efforts to mitigate plastic pollution," *Science,* vol. 369, no. 6510, 6510, pp. 1515-1518, Sep 18 2020, doi: 10.1126/science.aba3656.

[2] (2018). *EPA 530-F-20-007, Advancing Sustainable Materials Management: 2018 Fact Sheet*.

[3] D. Åkesson, T. Fuchs, M. Stöss, A. Root, E. Stenvall, and M. Skrifvars, "Recycling of wood fiber-reinforced HDPE by multiple reprocessing," *Journal of Applied Polymer Science,* vol. 133, no. 35, 2016, doi: 10.1002/app.43877.

[4] M. Kaci, A. Hamma, I. Pillin, and Y. Grohens, "Effect of Reprocessing Cycles on the Morphology and Properties of Poly(propylene)/Wood Flour Composites Compatibilized with EBAGMA Terpolymer," (in English), *Macromolecular Materials and Engineering,* vol. 294, no. 8, pp. 532-540, Aug 13 2009, doi: 10.1002/mame.200900089.

[5] A. Bourmaud and C. Baley, "Investigations on the recycling of hemp and sisal fibre reinforced polypropylene composites," (in English), *Polymer Degradation and Stability,* vol. 92, no. 6, pp. 1034-1045, Jun 2007, doi: 10.1016/j.polymdegradstab.2007.02.018.

[6] J. P. Correa-Aguirre, F. Luna-Vera, C. Caicedo, B. Vera-Mondragon, and M. A. Hidalgo-Salazar, "The Effects of Reprocessing and Fiber Treatments on the Properties of Polypropylene-Sugarcane Bagasse Biocomposites," *Polymers (Basel),* vol. 12, no. 7, Jun 27 2020, doi: 10.3390/polym12071440.

[7] M. R. N. Fazita, K. Jayaraman, D. Bhattacharyya, M. S. Hossain, M. K. M. Haafiz, and H. P. S. A. Khalil, "Disposal Options of Bamboo Fabric-Reinforced Poly(Lactic) Acid Composites for Sustainable Packaging: Biodegradability and Recyclability," (in English), *Polymers,* vol. 7, no. 8, pp. 1476-1496, Aug 2015, doi: 10.3390/polym7081465.

[8] A. Bourmaud, D. Akesson, J. Beaugrand, A. Le Duigou, M. Skrifvars, and C. Baley, "Recycling of L-Poly-(lactide)-Poly-(butylene-succinate)-flax biocomposite," (in English), *Polymer Degradation and Stability,* vol. 128, pp. 77-88, Jun 2016, doi: 10.1016/j.polymdegradstab.2016.03.018.

[9] M. Morreale, A. Liga, M. C. Mistretta, L. Ascione, and F. P. Mantia, "Mechanical, Thermomechanical and Reprocessing Behavior of Green Composites from Biodegradable Polymer and Wood Flour," *Materials (Basel),* vol. 8, no. 11, pp. 7536-7548, Nov 11 2015, doi: 10.3390/ma8115406.

[10] M. A. Fuqua, S. Huo, and C. A. Ulven, "Natural Fiber Reinforced Composites," *Polymer Reviews,* vol. 52, no. 3, pp. 259-320, 2012, doi: 10.1080/15583724.2012.705409.

[11] Q. H. Ji, X. J. Yu, A. G. A. Yagoub, L. Chen, and C. S. Zhou, "Efficient removal of lignin from vegetable wastes by ultrasonic and microwave-assisted treatment with ternary deep eutectic solvent," (in English), *Industrial Crops and Products,* vol. 149, Jul 2020, doi: 10.1016/j.indcrop.2020.112357.

[12] Y. D. Chen, Q. M. Wu, B. Huang, M. J. Huang, and X. L. Ai, "Isolation and Characteristics of Cellulose and Nanocellulose from Lotus Leaf Stalk Agro-wastes," (in English), *Bioresources,* vol. 10, no. 1, pp. 684-696, 2015. [Online]. Available: <Go to ISI>://WOS:000351941000057.

[13] R. Peretz, E. Sterenzon, Y. Gerchman, V. Kumar Vadivel, T. Luxbacher, and H. Mamane, "Nanocellulose production from recycled paper mill sludge using ozonation pretreatment followed by recyclable maleic acid hydrolysis," *Carbohydr Polym,* vol. 216, pp. 343-351, Jul 15 2019, doi: 10.1016/j.carbpol.2019.04.003.

[14] Q. Zhang, M. Zhao, Q. Xu, H. Ren, and J. Yin, "Enhanced Enzymatic Hydrolysis of Sorghum Stalk by Supercritical Carbon Dioxide and Ultrasonic Pretreatment," *Appl Biochem Biotechnol,* vol. 188, no. 1, pp. 101-111, May 2019, doi: 10.1007/s12010-018-2909-x.

[15] H. R. Amaral *et al.*, "Production of high-purity cellulose, cellulose acetate and cellulose-silica composite from babassu coconut shells," *Carbohydr Polym,* vol. 210, pp. 127-134, Apr 15 2019, doi: 10.1016/j.carbpol.2019.01.061.

[16] M. Karataş and N. Arslan, "Flow behaviours of cellulose and carboxymethyl cellulose from grapefruit peel," *Food Hydrocolloids,* vol. 58, pp. 235-245, 2016, doi: 10.1016/j.foodhyd.2016.02.035.

[17] M. Bakkal, M. S. Bodur, O. B. Berkalp, and S. Yilmaz, "The effect of reprocessing on the mechanical properties of the waste fabric reinforced composites," (in English), *Journal of Materials Processing Technology,* vol. 212, no. 11, pp. 2541-2548, Nov 2012, doi: 10.1016/j.jmatprotec.2012.03.008.

[18] Y. Cao *et al.*, "Combined bleaching and hydrolysis for isolation of cellulose nanofibrils from waste sackcloth," *Carbohydr Polym,* vol. 131, pp. 152-8, Oct 20 2015, doi: 10.1016/j.carbpol.2015.05.063.
[19] E. Espinosa, F. Rol, J. Bras, and A. Rodriguez, "Production of lignocellulose nanofibers from wheat straw by different fibrillation methods. Comparison of its viability in cardboard recycling process," (in English), *Journal of Cleaner Production,* vol. 239, Dec 1 2019, doi: 10.1016/j.jclepro.2019.118083.
[20] S. M. Yousefhashemi, A. Khosravani, and H. Yousefi, "Isolation of lignocellulose nanofiber from recycled old corrugated container and its interaction with cationic starch-nanosilica combination to make paperboard," (in English), *Cellulose,* vol. 26, no. 12, pp. 7207-7221, Aug 2019, doi: 10.1007/s10570-019-02562-2.
[21] R. J. Moon, G. T. Schueneman, and J. Simonsen, "Overview of Cellulose Nanomaterials, Their Capabilities and Applications," (in English), *Jom,* vol. 68, no. 9, pp. 2383-2394, Sep 2016, doi: 10.1007/s11837-016-2018-7.
[22] A. J. Benítez and A. Walther, "Cellulose nanofibril nanopapers and bioinspired nanocomposites: a review to understand the mechanical property space," *Journal of Materials Chemistry A,* vol. 5, no. 31, pp. 16003-16024, 2017, doi: 10.1039/c7ta02006f.
[23] H. Takagi and A. Asano, "Effects of processing conditions on flexural properties of cellulose nanofiber reinforced "green" composites," (in English), *Composites Part a-Applied Science and Manufacturing,* vol. 39, no. 4, pp. 685-689, 2008, doi: 10.1016/j.compositesa.2007.08.019.
[24] J. P. Lopez, J. Girones, J. A. Mendez, J. Puig, and M. A. Pelach, "Recycling Ability of Biodegradable Matrices and Their Cellulose-Reinforced Composites in a Plastic Recycling Stream," *Journal of Polymers and the Environment,* vol. 20, no. 1, pp. 96-103, 2011, doi: 10.1007/s10924-011-0333-1.
[25] L. J. Huang *et al.*, "Preparation and mechanical properties of modified nanocellulose/PLA composites from cassava residue," (in English), *Aip Advances,* vol. 8, no. 2, Feb 2018, doi: 10.1063/1.5023278.
[26] A. Abdulkhani, J. Hosseinzadeh, A. Ashori, S. Dadashi, and Z. Takzare, "Preparation and characterization of modified cellulose nanofibers reinforced polylactic acid nanocomposite," (in English), *Polymer Testing,* vol. 35, pp. 73-79, May 2014, doi: 10.1016/j.polymertesting.2014.03.002.
[27] J. Dong, C. T. Mei, J. Q. Han, S. Lee, and Q. L. Wu, "3D printed poly(lactic acid) composites with grafted cellulose nanofibers: Effect of nanofiber and post-fabrication annealing treatment on composite flexural properties," (in English), *Additive Manufacturing,* vol. 28, pp. 621-628, Aug 2019, doi: 10.1016/j.addma.2019.06.004.
[28] A. Dufresne, "Cellulose nanomaterials as green nanoreinforcements for polymer nanocomposites," *Philos Trans A Math Phys Eng Sci,* vol. 376, no. 2112, Feb 13 2018, doi: 10.1098/rsta.2017.0040.
[29] K. Y. Lee, Y. Aitomaki, L. A. Berglund, K. Oksman, and A. Bismarck, "On the use of nanocellulose as reinforcement in polymer matrix composites," (in English), *Composites Science and Technology,* vol. 105, pp. 15-27, Dec 10 2014, doi: 10.1016/j.compscitech.2014.08.032.
[30] M. Kattan, E. Dargent, J. Ledru, and J. Grenet, "Strain-induced crystallization in uniaxially drawn PETG plates," (in English), *Journal of Applied Polymer Science,* vol. 81, no. 14, pp. 3405-3412, Sep 29 2001, doi: DOI 10.1002/app.1797.
[31] R. B. Dupaix and M. C. Boyce, "Finite strain behavior of poly(ethylene terephthalate) (PET) and poly(ethylene terephthalate)-glycol (PETG)," (in English), *Polymer,* vol. 46, no. 13, pp. 4827-4838, Jun 17 2005, doi: 10.1016/j.polymer.2005.03.083.
[32] N. Vidakis *et al.*, "Sustainable Additive Manufacturing: Mechanical Response of Polyethylene Terephthalate Glycol over Multiple Recycling Processes," *Materials (Basel),* vol. 14, no. 5, Mar 2 2021, doi: 10.3390/ma14051162.

[33] G. J. P. Bex, B. L. J. Ingenhut, T. ten Cate, M. Sezen, and G. Ozkoc, "Sustainable approach to produce 3D-printed continuous carbon fiber composites: "A comparison of virgin and recycled PETG"," (in English), *Polymer Composites,* vol. 42, no. 9, pp. 4253-4264, Sep 2021, doi: 10.1002/pc.26143.
[34] P. Franciszczak, E. Piesowicz, and K. Kalnins, "Manufacturing and properties of r-PETG/PET fibre composite - Novel approach for recycling of PETG plastic scrap into engineering compound for injection moulding," (in English), *Compos Part B-Eng,* vol. 154, pp. 430-438, Dec 1 2018, doi: 10.1016/j.compositesb.2018.09.023.
[35] M. S. Bodur *et al.*, "The Effect of Reprocessing on the Tensile Properties of Composites," 2011.
[36] A. Soroudi and I. Jakubowicz, "Recycling of bioplastics, their blends and biocomposites: A review," (in English), *European Polymer Journal,* vol. 49, no. 10, pp. 2839-2858, Oct 2013, doi: 10.1016/j.eurpolymj.2013.07.025.
[37] C. Ngaowthong *et al.*, "Recycling of sisal fiber reinforced polypropylene and polylactic acid composites: Thermo-mechanical properties, morphology, and water absorption behavior," *Waste Manag,* vol. 97, pp. 71-81, Sep 2019, doi: 10.1016/j.wasman.2019.07.038.
[38] E. Uitterhaegen *et al.*, "Performance, durability and recycling of thermoplastic biocomposites reinforced with coriander straw," *Composites Part A: Applied Science and Manufacturing,* vol. 113, pp. 254-263, 2018, doi: 10.1016/j.compositesa.2018.07.038.
[39] L. Wang, J. Palmer, M. Tajvidi, D. J. Gardner, and Y. Han, "Thermal properties of spray-dried cellulose nanofibril-reinforced polypropylene composites from extrusion-based additive manufacturing," *Journal of Thermal Analysis and Calorimetry,* vol. 136, no. 3, pp. 1069-1077, 2018, doi: 10.1007/s10973-018-7759-9.
[40] A. R. Donovan and G. Moad, "A novel method for determination of polyester end-groups by NMR spectroscopy," (in English), *Polymer,* vol. 46, no. 14, pp. 5005-5011, Jun 27 2005, doi: 10.1016/j.polymer.2005.04.032.
[41] E. W. Fischer, H. J. Sterzel, and G. Wegner, "Investigation of the structure of solution grown crystals of lactide copolymers by means of chemical reactions," *Kolloid-Zeitschrift und Zeitschrift für Polymere,* vol. 251, no. 11, pp. 980-990, 1973, doi: 10.1007/bf01498927.
[42] X. Zhao *et al.*, "Recycling of natural fiber composites: Challenges and opportunities," (in English), *Resources, Conservation and Recycling,* vol. 177, Feb 2022, doi: 10.1016/j.resconrec.2021.105962.
[43] S. Bhattacharjee and D. S. Bajwa, "Degradation in the mechanical and thermo-mechanical properties of natural fiber filled polymer composites due to recycling," (in English), *Construction and Building Materials,* vol. 172, pp. 1-9, May 30 2018, doi: 10.1016/j.conbuildmat.2018.03.010.
[44] S. Bhattacharjee and D. S. Bajwa, "Feasibility of Reprocessing Natural Fiber Filled Poly(lactic acid) Composites: An In-Depth Investigation," *Advances in Materials Science and Engineering,* vol. 2017, pp. 1-10, 2017, doi: 10.1155/2017/1430892.
[45] Y. X. Yang, R. Boom, B. Irion, D. J. van Heerden, P. Kuiper, and H. de Wit, "Recycling of composite materials," (in English), *Chemical Engineering and Processing-Process Intensification,* vol. 51, pp. 53-68, Jan 2012, doi: 10.1016/j.cep.2011.09.007.
[46] L. Soccalingame *et al.*, "Reprocessing of artificial UV-weathered wood flour reinforced polypropylene composites," (in English), *Polymer Degradation and Stability,* vol. 120, pp. 313-327, Oct 2015, doi: 10.1016/j.polymdegradstab.2015.07.013.
[47] K. Copenhaver *et al.*, "Recycled Cardboard Containers as a Low Energy Source for Cellulose Nanofibrils and Their Use in Poly(L-lactide) Nanocomposites," (in English), *Acs Sustainable Chemistry & Engineering,* vol. 9, no. 40, pp. 13460-13470, Oct 11 2021, doi: 10.1021/acssuschemeng.1c03890.
[48] L. Wang, A. W. Roach, D. J. Gardner, and Y. Han, "Mechanisms contributing to mechanical property changes in composites of polypropylene reinforced with spray-dried cellulose nanofibrils," *Cellulose,* vol. 25, no. 1, pp. 439-448, 2017, doi: 10.1007/s10570-017-1556-7.

[49] Y. Peng, S. S. Nair, H. Y. Chen, N. Yan, and J. Z. Cao, "Effects of Lignin Content on Mechanical and Thermal Properties of Polypropylene Composites Reinforced with Micro Particles of Spray Dried Cellulose Nanofibrils," (in English), *Acs Sustainable Chemistry & Engineering,* vol. 6, no. 8, pp. 11078-11086, Aug 2018, doi: 10.1021/acssuschemeng.8b02544.

[50] Y. C. Peng, Y. S. Han, and D. J. Gardner, "Spray-Drying Cellulose Nanofibrils: Effect of Drying Process Parameters on Particle Morphology and Size Distribution," (in English), *Wood Fiber Sci,* vol. 44, no. 4, pp. 448-461, Oct 2012. [Online]. Available: <Go to ISI>://WOS:000310169400012.

[51] Y. Peng, D. J. Gardner, and Y. Han, "Drying cellulose nanofibrils: in search of a suitable method," *Cellulose,* vol. 19, no. 1, pp. 91-102, 2011, doi: 10.1007/s10570-011-9630-z.

[52] Y. C. Peng, S. A. Gallegos, D. J. Gardner, Y. Han, and Z. Y. Cai, "Maleic anhydride polypropylene modified cellulose nanofibril polypropylene nanocomposites with enhanced impact strength," (in English), *Polymer Composites,* vol. 37, no. 3, pp. 782-793, Mar 2016, doi: 10.1002/pc.23235.

[53] M. Jonoobi, J. Harun, A. P. Mathew, and K. Oksman, "Mechanical properties of cellulose nanofiber (CNF) reinforced polylactic acid (PLA) prepared by twin screw extrusion," (in English), *Composites Science and Technology,* vol. 70, no. 12, pp. 1742-1747, Oct 31 2010, doi: 10.1016/j.compscitech.2010.07.005.

[54] B. Madsen and H. Lilholt, "Physical and mechanical properties of unidirectional plant fibre composites - an evaluation of the influence of porosity," (in English), *Composites Science and Technology,* vol. 63, no. 9, pp. 1265-1272, Jul 2003, doi: 10.1016/S0266-3538(03)00097-6.

[55] F. R. Beltran, V. Lorenzo, J. Acosta, M. U. de la Orden, and J. Martinez Urreaga, "Effect of simulated mechanical recycling processes on the structure and properties of poly(lactic acid)," *J Environ Manage,* vol. 216, pp. 25-31, Jun 15 2018, doi: 10.1016/j.jenvman.2017.05.020.

[56] M. A. Elsawy, K. H. Kim, J. W. Park, and A. Deep, "Hydrolytic degradation of polylactic acid (PLA) and its composites," (in English), *Renew Sust Energ Rev,* vol. 79, pp. 1346-1352, Nov 2017, doi: 10.1016/j.rser.2017.05.143.

[57] N. Graupner, K. Albrecht, G. Ziegmann, H. Enzler, and J. Mussig, "Influence of reprocessing on fibre length distribution, tensile strength and impact strength of injection moulded cellulose fibre-reinforced polylactide (PLA) composites," (in English), *Express Polymer Letters,* vol. 10, no. 8, pp. 647-663, Aug 2016, doi: 10.3144/expresspolymlett.2016.59.

[58] P. Dhar, M. R. Kumar, S. M. Bhasney, P. Bhagabati, A. Kumar, and V. Katiyar, "Sustainable Approach for Mechanical Recycling of Poly(lactic acid)/Cellulose Nanocrystal Films: Investigations on Structure-Property Relationship and Underlying Mechanism," (in English), *Industrial & Engineering Chemistry Research,* vol. 57, no. 43, pp. 14493-14508, Oct 31 2018, doi: 10.1021/acs.iecr.8b02658.

[59] S. Chaitanya, I. Singh, and J. I. Song, "Recyclability analysis of PLA/Sisal fiber biocomposites," (in English), *Compos Part B-Eng,* vol. 173, Sep 15 2019, doi: 10.1016/j.compositesb.2019.05.106.

[60] D. Åkesson, T. Vrignaud, C. Tissot, and M. Skrifvars, "Mechanical Recycling of PLA Filled with a High Level of Cellulose Fibres," *Journal of Polymers and the Environment,* vol. 24, no. 3, pp. 185-195, 2016, doi: 10.1007/s10924-016-0760-0.

[61] G. M. Zhuo, X. L. Zhang, Y. T. Liu, and M. Wang, "Effect of multiple recycling on properties of poplar fiber reinforced high density polyethylene wood-plastic composites," (in English), *Materials Research Express,* vol. 6, no. 12, Dec 2019, doi: 10.1088/2053-1591/ab5742.

[62] M. L. Di Lorenzo, "Calorimetric analysis of the multiple melting behavior of poly(L-lactic acid)," *Journal of Applied Polymer Science,* vol. 100, no. 4, pp. 3145-3151, 2006, doi: 10.1002/app.23136.

[63] F. Hamonic, D. Prevosto, E. Dargent, and A. Saiter, "Contribution of chain alignment and crystallization in the evolution of cooperativity in drawn polymers," (in English), *Polymer,* vol. 55, no. 12, pp. 2882-2889, Jun 6 2014, doi: 10.1016/j.polymer.2014.04.030.

[64] T. T. Chen, W. K. Zhang, and J. Zhang, "Alkali resistance of poly(ethylene terephthalate) (PET) and poly(ethylene glycol-co-1,4-cyclohexanedimethanol terephthalate) (PETG) copolyesters: The role of composition," (in English), *Polymer Degradation and Stability,* vol. 120, pp. 232-243, Oct 2015, doi: 10.1016/j.polymdegradstab.2015.07.008.
[65] Y. H. Tsai, C. H. Fan, C. Y. Hung, and F. J. Tsai, "Amorphous copolyesters based on 1,3/1,4-cyclohexanedimethanol: Synthesis, characterization and properties," (in English), *Journal of Applied Polymer Science,* vol. 109, no. 4, pp. 2598-2604, Aug 15 2008, doi: 10.1002/app.28385.
[66] G. Sabbatier, D. Le Nouën, P. Chevallier, B. Durand, G. Laroche, and F. Dieval, "Air spun poly(lactic acid) nanofiber scaffold degradation for vascular tissue engineering: A 1H NMR study," *Polymer Degradation and Stability,* vol. 97, no. 8, pp. 1520-1526, 2012, doi: 10.1016/j.polymdegradstab.2012.04.017.
[67] M. T. Zell *et al.*, "Unambiguous Determination of the 13C and 1H NMR Stereosequence Assignments of Polylactide Using High-Resolution Solution NMR Spectroscopy," *Macromolecules,* vol. 35, no. 20, pp. 7700-7707, 2002, doi: 10.1021/ma0204148.
[68] S. R. Turner, "Development of amorphous copolyesters based on 1,4-cyclohexanedimethanol," *Journal of Polymer Science Part A: Polymer Chemistry,* vol. 42, no. 23, pp. 5847-5852, 2004, doi: 10.1002/pola.20460.
[69] N. González-Vidal, A. Martínez De Ilarduya, and S. Muñoz-Guerra, "Poly(ethylene-co-1,4-cyclohexylenedimethylene terephthalate) copolyesters obtained by ring opening polymerization," *Journal of Polymer Science Part A: Polymer Chemistry,* vol. 47, no. 22, pp. 5954-5966, 2009, doi: 10.1002/pola.23639.
[70] K. Tanaka, M. Oouchi, F. Hayashi, H. Maeda, and H. Waki, "Structural Analysis of the End Groups and Substructures of Commercial Poly(ethylene terephthalate) by Multiple-WET 1H/13C NMR," *Macromolecules,* vol. 49, no. 15, pp. 5750-5754, 2016, doi: 10.1021/acs.macromol.6b01105.
[71] K. Nobuta *et al.*, "Characterization of cellulose nanofiber sheets from different refining processes," *Cellulose,* vol. 23, no. 1, pp. 403-414, 2015, doi: 10.1007/s10570-015-0792-y.
[72] Y. Okahisa, Y. Furukawa, K. Ishimoto, C. Narita, K. Intharapichai, and H. Ohara, "Comparison of cellulose nanofiber properties produced from different parts of the oil palm tree," *Carbohydr Polym,* vol. 198, pp. 313-319, Oct 15 2018, doi: 10.1016/j.carbpol.2018.06.089.
[73] J. Gong, J. Li, J. Xu, Z. Xiang, and L. Mo, "Research on cellulose nanocrystals produced from cellulose sources with various polymorphs," *RSC Advances,* vol. 7, no. 53, pp. 33486-33493, 2017, doi: 10.1039/c7ra06222b.
[74] C. D. M. Dominic *et al.*, "Cellulose Nanofibers Isolated from the Cuscuta Reflexa Plant as a Green Reinforcement of Natural Rubber," *Polymers (Basel),* vol. 12, no. 4, Apr 4 2020, doi: 10.3390/polym12040814.